Molecular Crystals and Liquid Crystals
Publication details, including instructions for authors and subscription information:
http://www.tandfonline.com/loi/gmcl16

Unusual Glassy Smectic-G Liquid Crystal: Heat Capacity of N-p-n-Pentyloxybenzylidene-p'-n-butylaniline between 11 and 393 K

M. Sorai [a] , K. Tani [a] & H. Suga [a]
[a] Chemical Thermodynamics Laboratory and Department of Chemistry, Faculty of Science, Osaka University, Toyonaka, Osaka, 560, Japan
Version of record first published: 17 Oct 2011.

To cite this article: M. Sorai , K. Tani & H. Suga (1983): Unusual Glassy Smectic-G Liquid Crystal: Heat Capacity of N-p-n-Pentyloxybenzylidene-p'-n-butylaniline between 11 and 393 K, Molecular Crystals and Liquid Crystals, 97:1, 365-386

To link to this article: http://dx.doi.org/10.1080/00268948308073164

Mol. Cryst. Liq. Cryst., 1983, vol. 97, pp. 365–386
0026-8941/83/9704–0365/$18.50/0

Printed in the United States of America

Unusual Glassy Smectic-G Liquid Crystal: Heat Capacity of *N-p-n*-Pentyloxybenzylidene-*p'-n*-butylaniline between 11 and 393 K†

M. SORAI, K. TANI and H. SUGA

Chemical Thermodynamics Laboratory and Department of Chemistry, Faculty of Science, Osaka University, Toyonaka, Osaka 560, Japan

(Received February 2, 1983)

The heat capacities of the title compound ($C_5H_{11}O—C_6H_4—CH=N—C_6H_4—C_4H_9$, abbreviation 5O · 4) with a purity of 99.92 mole percent have been measured with an adiabatic-type calorimeter between 11 and 393 K. The transition temperature and the enthalpy and entropy of phase transition for stable crystal → S_G, S_G → N and N → isotropic liquid were T_c = 299.69 K/ΔH = 22.68 kJ mol^{-1}/ΔS = 75.70 J K^{-1} mol^{-1}, 325.72/7.11/21.79 and 342.48/1.78/5.22, respectively. The crystal which melts at 285.5 K is a metastable modification. The S_A phase hitherto reported in between S_G and N does not exist. The glassy S_G state was realized by rapid cooling of the specimen from the S_G phase. The molar enthalpy of the glassy S_G state at 0 K was by (10.1 ±0.1) kJ mol^{-1} higher than that of the stable crystalline state and the residual entropy of the glassy state was (9.40 ±0.83) J K^{-1} mol^{-1}. The relaxational heat-capacity anomaly was observed from as low as 100 K and double glass transition phenomenon occurred around 200 K; a quite unusual phenomenon which has never been observed for the glassy states of nematic and cholesteric liquid crystals. The present results give a fair evidence that the unusual glass transition phenomenon previously found for the S_G state of 6O · 4 (a homologous compound) is not exceptional at all but common to the smectic glasses; at least common to the glassy S_G states. Two possible origins responsible for the double glass transitions have been discussed.

1. INTRODUCTION

The glass transition phenomenon of the smectic glasses is known to be unusual in the sense that the temperature range of glass transition is extraor-

†Contribution No. 53 from Chemical Thermodynamics Laboratory. Presented at the Ninth International Liquid Crystal Conference. Bangalore, 1982.

dinarily wide.[1] The heat capacity measurements for the glassy S_G state of *N-p-n*-hexyloxybenzylidene-*p'-n*-butylaniline (abbreviated as 6O · 4) revealed that this is due to double glass transitions which occur successively.[2,3] Since this kind of double glass transition phenomenon has never been observed for the cholesteric,[4] nematic[1,5,6] and isotropic-liquid[1,6] glasses, we anticipated that it might be caused by layer structures inherent in smectic liquid crystals.[2,3] If this is the case, similar phenomenon should commonly be observed for other types of smectic liquid crystals such as S_A, S_B, S_C, *etc*. From an experimental viewpoint, it is urgent to accumulate such circumstantial evidences. The main purpose of the present paper is to examine, based on heat capacity measurements, whether the double glass transition phenomenon will present itself in the S_G state of compounds other than 6O · 4. The compound studied here is *N-p-n*-pentyloxybenzylidene-*p'-n*-butylaniline (denoted as 5O · 4), for which the glassy smectic state is known to be easily realized.[1]

The phase sequence of 5O · 4 hitherto reported is summarized as follows:

K 24 S_{II} 52 S_I 54 N 71 IL	(DTA[7]),
K 12 S_B 52.1 S_A 52.4 N 69.0 IL	(DSC[8,9]),
K 9 S 48 N 68 IL	(DTA[1]),
K 34 S_G 52 S_A 52.4 N 68.7 IL	(DSC[10]),
K 20 S_G 51.9 S_A 52.4 N 69.2 IL	(microscope[10]),
K 12 S_G 53 S_A 53.5 N 70 IL	(microscope[11]),

where the linear notation of Verbit[12] is adopted and transition temperatures are represented in Celsius' scale. Recent assignment[10,11] of the smectic phase adjacent to the crystalline phase is S_G, hence the previous notations (S_{II}[7], S_B[8,9] and S[1]) should be read as S_G. Strangely, the melting points are scattered in the wide range from 9 to 34°C and the S_A phase has not been detected only in our case.[1] To elucidate these unclear aspects of 5O · 4 is also one of the present purposes.

2. EXPERIMENTAL

The sample was synthesized by azeotropic dehydration of *p-n*-amyloxybenzaldehyde and *p-n*-butylaniline in a benzene solution by removing the water produced. The crude product was purified by recrystallization from absolute ethanol four times and then by molecular distillation under a vacuum.

Heat capacity measurements were made with an adiabatic-type calorimeter[13] between 11 and 393 K. A calorimeter cell made of gold and platinum[14] contained the specimen of 19.2191 g (≙0.0594141 mol) and a small amount of helium gas to aid the heat transfer inside the cell.

To estimate the contribution of intramolecular vibrations to the heat capacity, the infrared absorption spectra in the range 4000–30 cm^{-1} were recorded.

For identification of the mesophases, optical textures were observed under a polarization microscope (Olympus, Model BHA-751-P) equipped with a heating stage (Union Optical Co., Ltd., Model CMS-2).

3. RESULTS

The results of preliminary experiment to roughly identify the melting point are shown in Figures 1a and b, in which the temperature rise of the calorimeter due to continuous heating is plotted as a function of time. In run (a), prior to the measurement, the calorimeter was once cooled rapidly from 320 to 80 K, while in run (b) the precooling rate was rather slow. Upon continuous heating, the former gave rise to a crystallization from the undercooled S_G state at around 230 K and the resulting crystal isothermally melted at 285.5 K (Figure 1a). Independently of the precooling rate, the latter likewise showed a melting phenomenon at the same temperature (Figure 1b).

Now that the melting point of 5O · 4 was found to be 285.5 K, we annealed the specimen at around 282 K for 4 days to obtain well-grown crystals in thermal equilibrium. Heat capacity measurements for the specimen thus treated, however, did not show the melting at 285.5 K. Instead, a new melting phenomenon was observed at 299.6 K. This fact obviously indicates that the crystal melted at 285.5 K (=12.3°C) belongs to a metastable modification while the crystal melted at 299.6 K (=26.4°C) is a more stable one. It seems, therefore, that the low melting points (9 and 12°C) hitherto reported[1,8,9,11] correspond to melting of the metastable crystal whereas the high values (20, 24 and 34°C)[7,10] are due to melting of the stable one.

The results of the heat capacity measurements were evaluated in terms of C_p, the molar heat capacity at constant pressure, and plotted in Figure 2. A listing of the experimental data is given in Table I.

As it took a long time to obtain the stable crystal we began with heat capacity measurements for the mesomorphic and isotropic liquid phases (series 1, 2, 4, 5, 7 and 9). Special attention was paid to see whether the S_A phase exists in between the S_G and N phases as has been reported.[7–11] As shown in Figure 3, however, in spite of careful and repeating measurements the present results did not exhibit even a trace of the S_A phase; namely, the S_G phase was directly transformed into the N phase at 325.72 K. What differs from dynamic thermal analyses such as DTA and

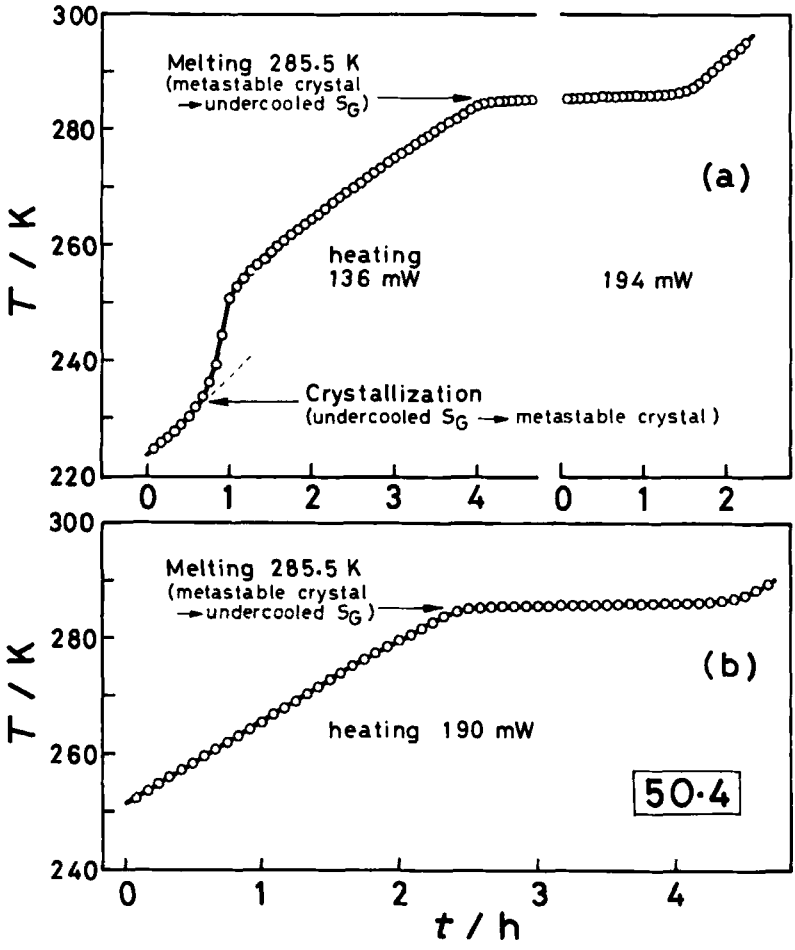

FIGURE 1 The temperature rise of the calorimeter due to continuous heating is plotted as a function of temperature. (a) Prior to the measurement, the calorimeter was once cooled rapidly from 320 to 80 K. During the melting process, the electric power was changed from 136 to 194 mW. (b) Continuous heating of the specimen once cooled slowly from 320 to 80 K.

DSC is that the adiabatic calorimetry is a static or equilibrium method; resolutions of the temperature are much higher in the calorimetry than in thermal analyses. Therefore, it is not likely that the present measurements have failed to detect the S_A phase, if any. Further evidence of absence of the S_A phase was given by microscopic observations; only a mosaic texture characteristic of S_G state and a schlieren texture of N state were observed both on cooling and heating. A plausible reason to account for the incom-

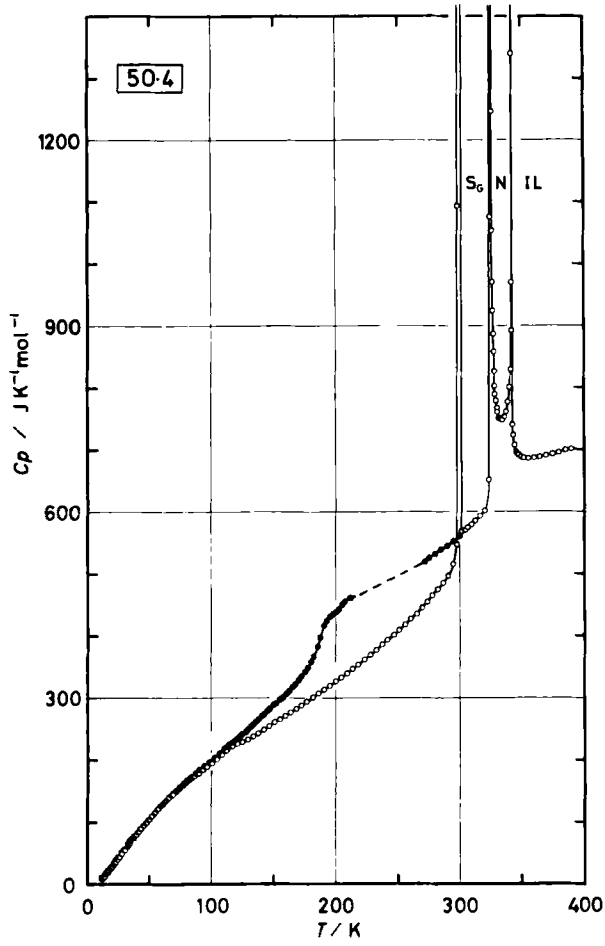

FIGURE 2 Molar heat capacity of 50 · 4. ○: The stable phases. ●: The glassy and undercooled S_G phases.

patibility with the reported data seems to be purity of the specimen because the sample, which did not exhibit the S_A phase,[1] showed a small shoulder on the high temperature side of the main peak of DTA after storing it in a refrigerator for 8 years, during which a partial hydrolysis might occur. Purity of the present calorimetric sample freshly prepared was 99.92 mole percent from a fractional fusion method.

The heat capacity of the glassy S_G state were measured in series 3 and 6 for the specimen cooled from 320 K to 10 and 96 K at an average rate of 6.4 and 3.5 K min^{-1}, respectively. As shown in Figure 2 by solid

TABLE I

Molar heat capacity of *N-p-n*-pentyloxybenzylidene-*p'*-*n*-butylaniline

T/K	C_p/J K^{-1} mol^{-1}	T/K	C_p/J K^{-1} mol^{-1}	T/K	C_p/J K^{-1} mol^{-1}
ΔH measurement		342.536	2710.2	16.736	23.375
320.91 → 333.48 K		342.748	740.87	17.798	26.113
Series 1[a,b]		343.285	723.27	18.873	28.858
292.861	549.13	344.184	707.67	20.089	31.870
295.585	553.09	345.363	696.60	21.463	35.636
298.406	557.90	347.329	692.20	23.022	39.694
302.017	563.92	349.957	687.91	24.665	44.041
306.409	570.93	Series 2[b]		26.258	48.630
310.763	578.03	304.332	570.69	27.894	52.780
315.078	586.66	306.898	574.82	31.363	61.256
319.350	596.12	309.452	579.03	33.018	65.799
322.170	603.82	312.623	585.49	34.634	70.178
322.765	626.63	316.401	592.66	36.239	74.150
323.340	677.67	320.150	601.47	37.915	78.268
323.857	880.70	323.194	651.33	39.658	82.513
324.281	1213.4	324.512	1076.1	40.812	85.128
324.619	1621.3	324.754	1511.5	41.542	86.946
324.886	2206.8	324.944	1970.9	42.900	90.156
325.091	3013.2	325.098	2521.1	45.067	94.916
325.249	4044.6	325.168	3006.9	47.305	99.725
325.370	5431.2	325.250	3554.5	49.551	104.54
325.463	7039.4	325.343	4454.7	51.890	109.80
325.536	8969.3	325.420	5477.8	54.344	115.11
325.595	11151.	325.484	6654.6	56.892	121.55
325.643	13909.	325.537	7931.1	59.568	127.18
325.708	6659.0	325.583	9439.6	62.360	132.30
325.867	2215.2	325.622	10997.	65.188	137.73
326.298	1078.3	325.656	11989.	66.287	140.93
326.844	907.86	325.687	13882.	68.008	143.43
327.317	857.46	325.715	14780.	69.121	146.28
327.805	826.08	325.744	13229.	71.969	151.68
328.303	803.88	325.814	3278.3	74.878	157.21
328.809	789.90	325.944	2392.2	77.857	162.50
329.417	779.47	326.142	1246.9	80.886	167.97
330.126	767.79	326.407	1053.3	83.988	173.37
330.841	761.42	326.697	971.12	87.228	179.08
332.726	751.23	327.000	924.82	90.663	184.68
333.746	749.22	327.314	886.61	94.309	191.01
334.764	748.59	327.635	858.51	98.203	197.47
336.033	753.66			102.230	203.94
337.547	762.03	Cooled rapidly		106.784	211.17
339.045	777.09	from 320 K to 10 K		110.825	218.78
340.275	801.19	Series 3[c,a]		114.895	225.51
341.100	830.01	11.877	11.840	119.022	232.00
341.762	892.30	12.710	13.364	123.184	239.19
342.193	970.30	13.552	15.666	127.371	245.61
342.386	1340.5	14.526	18.078	131.603	254.33
342.480	18243.	15.607	20.724	135.910	262.33

TABLE I *(Continued)*

T/K	C_p/J K^{-1} mol^{-1}	T/K	C_p/J K^{-1} mol^{-1}	T/K	C_p/J K^{-1} mol^{-1}
140.256	270.28	335.594	750.52	325.545	8469.2
144.933	278.93			325.607	10488.
149.948	288.30	ΔH measurement		325.657	13776.
155.006	297.96	336.40 K → 345.43 K		325.693	14120.
160.084	307.51	Series 5[b]		325.720	14806.
165.154	318.32	346.733	693.24	325.799	2729.5
170.216	329.71	349.353	688.46	326.000	1842.0
175.271	342.82			326.345	1054.7
180.331	358.70	Cooled rapidly from			
185.343	382.83	320 K to 96 K		Cooled to 270 K	
190.291	416.60	Series 6[c,a]		Series 8[a]	
195.213	431.43	112.504	221.36	271.192	519.54
200.133	439.34	116.663	228.65	274.696	525.11
205.049	450.57	120.731	235.71	279.857	532.12
209.900	463.58	124.816	242.46	284.842	539.17
214.735	465.82	129.008	249.40	289.777	545.71
219.579	480.54	133.278	257.48	294.745	552.81
		137.619	265.34	299.778	560.63
ΔH measurement		142.146	273.55	Series 9[b]	
221.96 K → 315.45 K		147.004	282.58	346.436	695.67
Series 4[b]		152.057	291.89	349.046	691.63
317.819	593.41	157.132	301.61	351.785	686.70
321.474	605.41	162.212	311.73	355.473	686.06
324.132	1045.3	167.283	322.52	360.032	686.62
325.047	2505.8	172.337	334.53	364.775	688.42
325.173	3121.9	177.411	348.67	369.763	690.29
325.278	3857.3	182.474	366.37	374.795	693.16
325.365	4735.0	187.475	397.30	379.817	695.97
325.437	5862.0	192.415	424.46	384.825	698.62
325.497	6914.1	197.334	435.42	389.813	700.93
325.548	8434.4	202.267	442.57		
325.592	9663.6	207.168	455.68	Annealed at 297 K	
325.630	11567.	212.009	461.70	for 8 days and then	
325.662	12843.	216.837	470.57	cooled slowly to	
325.691	15020.			11 K	
325.717	16694.	ΔH measurement		Series 10[b]	
325.762	5835.7	214.43 K → 301.81 K		12.061	9.407
325.861	2670.4	Series 7[b]		13.039	11.679
326.040	1415.6	304.009	567.59	14.088	13.782
326.291	1082.4	308.396	574.11	15.242	16.612
326.856	913.35	312.745	582.46	16.458	19.576
327.405	856.12	317.050	591.36	17.684	22.758
328.049	817.20	321.305	605.74	18.970	25.590
328.749	793.99	323.986	830.39	20.233	28.840
329.552	777.11	324.493	1310.7	21.552	32.219
330.415	764.47	324.807	1836.9	23.073	36.110
331.284	757.37	325.047	2567.5	24.664	40.311
332.218	754.15	325.227	3570.1	26.205	44.464
333.217	748.95	325.362	4845.9	27.701	48.475
334.254	746.71	325.465	6456.0	28.048	49.166

TABLE I *(Continued)*

T/K	C_p/J K^{-1} mol^{-1}	T/K	C_p/J K^{-1} mol^{-1}	T/K	C_p/J K^{-1} mol^{-1}
29.210	53.091	96.785	189.69	227.912	369.79
29.579	52.871	100.687	195.16	232.488	377.37
30.734	56.082	104.431	201.33	237.063	385.50
31.100	56.995	108.484	208.49	241.640	393.29
32.676	61.500	112.541	215.55	246.216	401.30
34.329	66.160	116.595	222.28	250.787	409.75
36.033	70.749	120.687	226.58	255.351	418.51
37.800	75.344	124.860	229.02	259.902	427.40
39.747	80.403	129.050	232.99	264.863	435.33
41.809	85.590	133.226	237.98	269.168	445.12
43.866	90.652	137.425	243.13	273.462	454.72
46.005	95.551	142.117	248.96	277.747	464.39
48.213	100.57	146.366	254.43	282.027	474.84
50.417	105.65	150.674	260.26	286.299	485.21
52.719	111.05	155.018	265.36	290.559	497.42
55.142	116.63	159.386	270.81	294.812	515.96
57.666	122.34	163.762	276.53	297.381	546.39
60.283	127.94	168.135	282.32	298.550	1093.7
61.274	129.52	172.501	288.15	299.486	12592.
63.825	134.53	176.861	294.07	299.606	56132.
66.485	139.45	181.753	300.92	299.638	119680.
69.239	144.68	186.214	307.15	299.656	181640.
72.045	149.73	190.792	313.50	299.668	254300.
74.882	154.62	195.389	319.96	299.676	373980.
77.730	159.41	199.992	326.64	299.682	403930.
80.690	164.43	204.564	333.24	299.692	190980.
83.724	169.30	209.124	339.80	300.098	2755.3
86.789	174.36	213.700	346.74	301.789	568.13
90.007	179.28	218.279	353.91	304.369	570.82
93.369	184.49	223.361	362.11	306.940	574.70

[a]Undercooled S_G phase [b]Stable phase [c]Glassy S_G phase

circles, the behavior of the glassy S_G state bears a close resemblance to that of 6O • 4:[2,3] widely spread excess heat capacities and the existence of two stepped anomalies at around 200 K.

When the temperature of the specimen reached about 220 K, a vast evolution of heat was observed due to an irreversible transition from the undercooled S_G to the metastable crystalline phase. In order to correlate the enthalpy of the glassy S_G state with that of the stable crystal, the temperature rise due to the crystallization was followed while keeping adiabatic conditions of the calorimeter, and then the known amount of electric energy was supplied till the calorimeter reached 315.45 K, a temperature well above the melting point of the stable crystal.

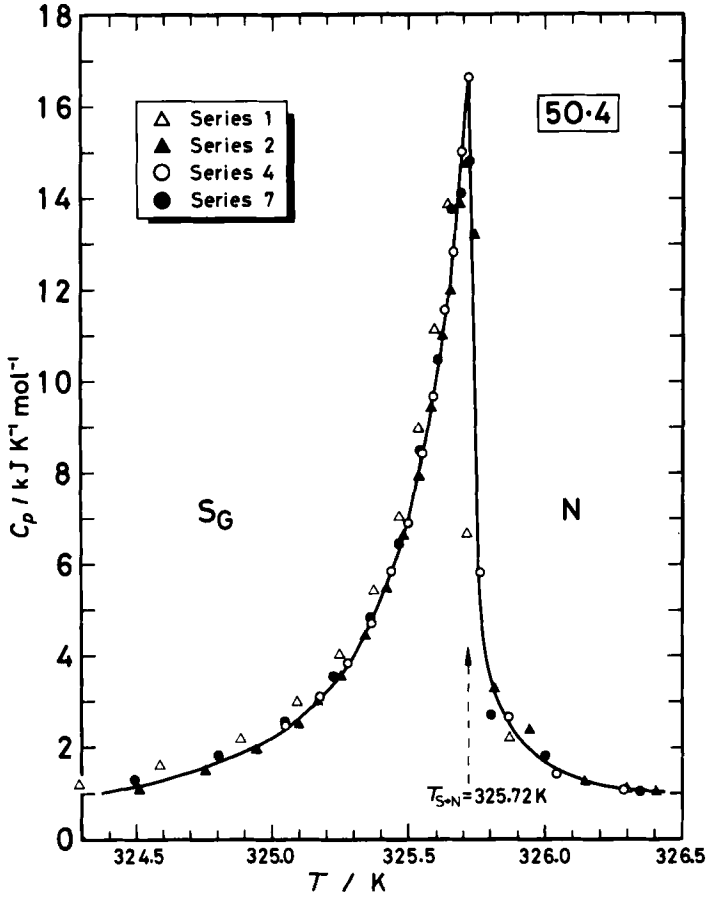

FIGURE 3 Molar heat capacity of 5O · 4 in the vicinity of the phase transition from S_G to N.

The C_p values in a high-temperature region of the undercooled S_G state were measured in series 1 and 8 for the specimen slowly cooled from the N state to 290 and 270 K, respectively. Further cooling brought about spontaneous crystallization, which interrupted the heat capacity measurements. It should be noted here that the C_p values of the S_G phase realized *via* the stable crystal (series 2 and 10) were systematically by about 2.5 J K^{-1} mol^{-1} higher than those of the S_G phase obtained by cooling from the N phase (series 1 and 8). This fact may be interpreted in terms of the short-range order characteristic of crystal, which might be present in the former but absent in the latter.

Prior to the heat capacity measurements for the stable crystalline phase (series 10), the specimen once cooled to 150 K was annealed at 297 K for 8 days and then slowly cooled to 11 K. The results of the measurements showed a small hump centered at 117 K and spread over the region from 70 to 140 K. The time required for thermal equilibration after an energy input was not elongated in this temperature region. Therefore, this hump should be regarded as a simple heat capacity anomaly rather than a phase transition. In order to determine the excess thermodynamic quantities due to this hump, a 'normal' heat capacity curve was estimated according to an effective frequency spectrum method[15] by using the infrared absorption data of 32 modes (96 degrees of freedom) between 3040 and 545 cm^{-1}. The 'best' frequency spectrum reproduced 35 C_p data in the range 12.1–69.2 K and 15 C_p data in the range 137.4–200.0 K within ± 0.53 $J K^{-1} mol^{-1}$. The excess heat capacities, ΔC_p, beyond this normal curve are plotted in Figure 4. The maximum value of ΔC_p was only 7 $J K^{-1} mol^{-1}$ at 117 K, while the excess enthalpy and entropy were $\Delta H_{exc} = 153$ J mol^{-1} and $\Delta S_{exc} = 1.33$ $J K^{-1} mol^{-1}$, respectively. Judging from the excess entropy, we cannot deny a possibility that rotational disorder of the methyl-constituent of the pentyloxy group is responsible for the present anomaly.

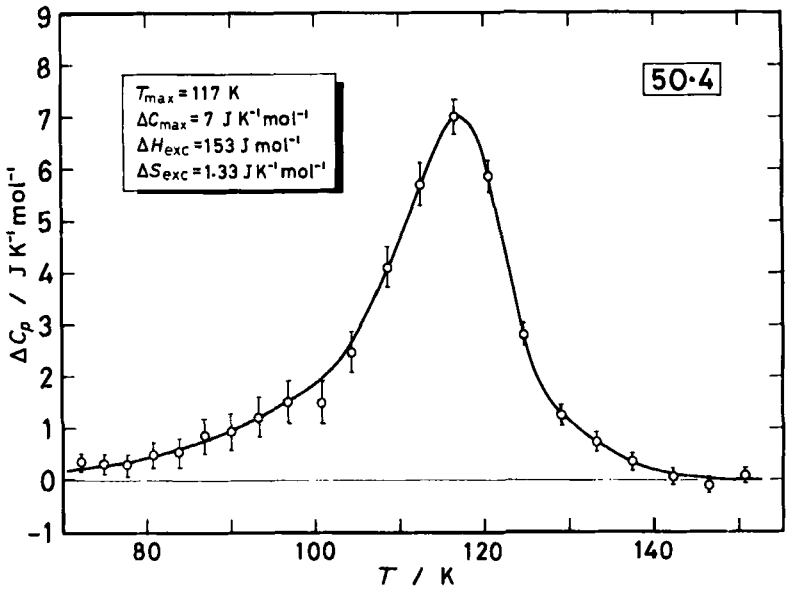

FIGURE 4 Heat capacity anomaly at around 120 K. ΔC_p means the excess part beyond the normal heat capacity.

The thermodynamic functions of 5O · 4 for the stable phases were calculated from the heat capacity data and the calorimetric enthalpy measurements across the respective phase transitions. The heat capacity below 11 K was estimated on the basis of the 'normal' heat capacity mentioned above. Table II contains a listing of values for the heat capacity, C_p^o, the entropy, S^o, the enthalpy function, $(H^o - H_0^o)/T$ and the Gibbs energy function, $-(G^o - H_0^o)/T$, at selected temperatures.

The heat capacity of the glassy S_G state below 11 K was similarly estimated from an effective frequency method by using 45 C_p data in the range 11.9–98.2 K and the same infrared absorption data as those of the crystal. The heat capacity of the undercooled S_G state in the range from 220 to 270 K, over which no C_p measurements were made, was evaluated by

TABLE II

Standard thermodynamic functions for the stable phases of *N*-*p*-*n*-pentyloxybenzylidene-*p'*-*n*-butylaniline in J K^{-1} mol^{-1} (relative molecular mass 323.477)

T/K	C_p°	S°	$(H^\circ - H_0^\circ)/T$	$-(G^\circ - H_0^\circ)/T$
5	(1.14)	(0.435)	(0.317)	(0.118)
10	(6.31)	(2.559)	(1.836)	(0.723)
20	28.24	13.030	9.123	3.907
30	54.64	29.439	19.867	9.572
40	81.04	48.759	31.876	16.883
50	104.69	69.437	44.123	25.314
60	127.34	90.562	56.149	34.413
70	146.05	111.59	67.640	43.945
80	163.26	134.89	81.226	53.665
90	179.27	152.39	88.860	63.530
100	194.20	172.07	98.661	73.408
120	225.86	210.42	117.37	93.050
140	246.33	246.59	134.14	112.45
160	271.61	281.14	149.77	131.37
180	298.47	314.67	164.77	149.89
200	326.65	347.38	179.55	167.83
220	356.69	379.89	194.25	185.64
240	390.50	412.36	209.18	203.18
260	427.56	445.04	224.52	220.52
280	469.89	478.16	240.42	237.75
Transition from crystal to smectic-G at 299.69 K				
310	580.15	606.76	340.72	266.05
320	595.00	625.50	348.52	276.98
Transition from smectic-G to nematic at 325.72 K				
340	795.80	686.97	387.47	299.49
Transition from nematic to isotropic liquid at 342.48 K				
360	686.61	729.30	407.04	322.26
380	696.06	766.65	421.98	344.67
390	701.52	784.80	429.07	355.72

referring to the enthalpy diagram so that the area under the assumed C_p curve in this temperature range may coincide with the enthalpy difference between these two temperatures. The heat capacity thus estimated is given by the following equation,

$$[C_p \text{ (undercooled } S_G) - C_p \text{ (crystal)}]/\text{J K}^{-1}\,\text{mol}^{-1} = 5.7915 \times 10^{-3}T^2 - 3.6463T + 632.80 \quad (220 \leq T/\text{K} \leq 270), \qquad (1)$$

and illustrated in Figure 2 by a broken line. The thermodynamic functions for the glassy and undercooled S_G states are listed in Table III, in which a reference state of the enthalpy at 0 K has been taken as that of the crystal, H_0° (crystalline).

TABLE III

Thermodynamic functions for the glassy and undercooled S_G phases of *N*-*p*-*n*-pentyloxybenzylidene-*p'*-*n*-butylaniline in J K^{-1} mol^{-1}: H_0° means the enthalpy of the stable crystalline phase at 0 K

T/K	C_p°	S°	$(H^\circ - H_0^\circ)/T$	$-(G^\circ - H_0^\circ)/T$
	$S_0^\circ = (9.40 \pm 0.83)$ J K^{-1} mol^{-1}			
	H_0° (glassy S_G) $- H_0^\circ$ (crystalline) $= (10.1 \pm 0.1)$ kJ mol^{-1}			
5	(1.94)	(10.301)	(2029.9)	(−2019.5)
10	(8.19)	(13.266)	(1017.2)	(−1004.0)
20	31.65	25.754	518.32	−492.57
30	57.73	43.628	360.55	−316.92
40	83.32	63.821	288.12	−224.30
50	105.55	84.832	249.42	−164.59
60	127.97	106.08	227.34	−121.26
70	147.94	127.25	214.50	−87.25
80	166.37	148.22	207.36	−59.14
90	183.60	168.83	203.79	−34.96
100	200.36	189.06	202.60	−13.55
120	234.12	228.53	205.03	23.50
140	269.81	267.24	211.69	55.55
160	307.34	305.81	221.40	84.41
180	357.56	344.80	233.64	111.16
200	439.15	387.65	251.02	136.63
220[a]	467.61	431.41	269.93	161.48
240[a]	481.78	472.65	286.94	185.71
260[a]	503.83	512.02	302.72	209.30
280	532.32	550.35	318.07	232.28
300	561.46	588.03	333.29	254.74
310[b]	(580.15)	(606.76)	(340.72)	(266.05)

[a]The values at these temperatures are estimated on the basis of the interpolation curve, Eq. 1.

[b]The values at this temperature correspond to those for the stable smectic-G phase.

4. ENTHALPY AND ENTROPY OF PHASE TRANSITION

To separate the enthalpy and entropy associated with the phase transitions, we approximated normal heat capacities, C_p (normal), for crystal, S_G and isotropic-liquid by straight lines so that they may coincide with the slopes of the C_p *vs* T curve in the temperature regions far from the transition points (see Figure 5). The C_p (normal) for the N phase is a straight line simply connecting C_p (normal, S_G) at $T_C(S_G \rightarrow N)$ and C_p (normal, IL) at T_C ($N \rightarrow IL$). The estimated normal heat capacities are given by the following equations,

$$\left.\begin{aligned}
&\text{(A)}\quad C_p\,(\text{normal, K})/\text{J K}^{-1}\,\text{mol}^{-1} = 2.3491\,T - 187.67 \\
&\qquad\qquad (T/\text{K} \leq 299.69), \\
&\text{(B)}\quad C_p\,(\text{normal, S}_G)/\text{J K}^{-1}\,\text{mol}^{-1} = 1.7793\,T + 28.88 \\
&\qquad\qquad (299.69 \leq T/\text{K} \leq 325.72), \\
&\text{(C)}\quad C_p\,(\text{normal, N})/\text{J K}^{-1}\,\text{mol}^{-1} = 4.0243\,T - 702.36 \\
&\qquad\qquad (325.72 \leq T/\text{K} \leq 342.48), \\
&\text{(D)}\quad C_p\,(\text{normal, IL})/\text{J K}^{-1}\,\text{mol}^{-1} = 0.53349\,T + 493.17 \\
&\qquad\qquad (342.48 \leq T/\text{K}),
\end{aligned}\right\} \quad (2)$$

and illustrated in Figure 5 by broken lines.

The enthalpy, ΔH, and entropy, ΔS, of transition were determined by integrating the excess heat capacity beyond these base lines with respect to T and ln T, respectively. For these calculations, the results of the calorimetric enthalpy measurements across the respective phase transitions were also taken into account. The thermodynamic data concerning the phase transitions are summarized in Table IV. The large $\Delta S(S_G \rightarrow N)$ value of 21.79 J K^{-1} mol^{-1} gives a definite evidence from a thermodynamic viewpoint that molecular arrangement is of very high order in the S_G state as has been ascertained from structural studies.[16–18]

If we compare the present results with those of 6O · 4,[2,3] we perceive interesting facts. Firstly, the $\Delta S(S_G \rightarrow N)$ of 21.79 J K^{-1} mol^{-1} is essentially equal to the sum (22.04 J K^{-1} mol^{-1}) of $\Delta S(S_G \rightarrow S_B)$, $\Delta S(S_B \rightarrow S_A)$ and $\Delta S(S_A \rightarrow N)$ found for 6O · 4. This fact indicates that the transition entropies balance independently of the intermediate phases on the path if the initial and final phases are respectively the same. Secondly, the $\Delta S(N \rightarrow IL)$ of 5.22 J K^{-1} mol^{-1} is in good agreement with 5.37 J K^{-1} mol^{-1} for 6O · 4. Thirdly, the $\Delta S(K \rightarrow S_G)$ of 75.70 J K^{-1} mol^{-1} agrees well with 75.98 J K^{-1} mol^{-1} of 6O · 4. In other words, the cumulative transition entropy of 102.7 J K^{-1} mol^{-1} for 5O · 4 is substantially the

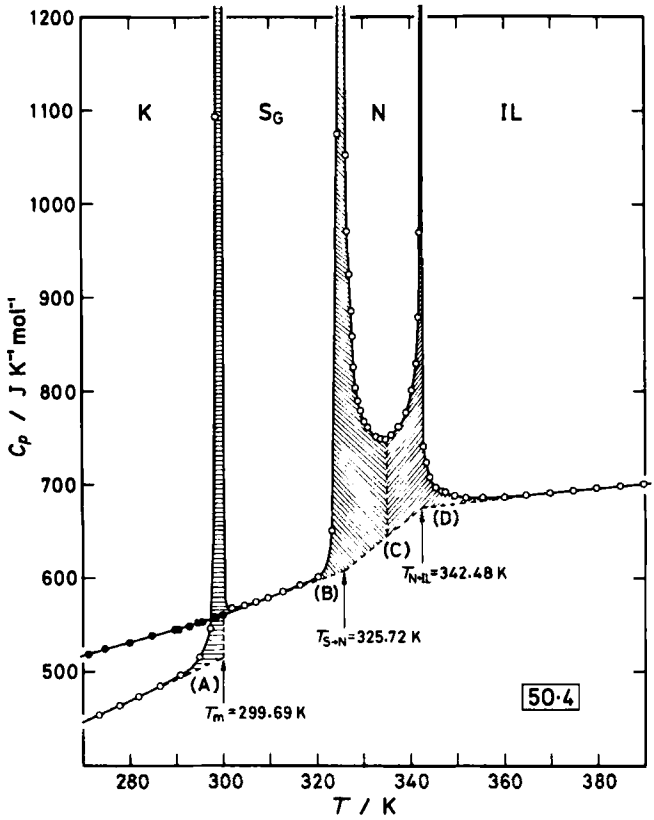

FIGURE 5 Molar heat capacity of 5O · 4 in the vicinity of phase transitions. Broken lines labelled (A), (B), (C) and (D) are given in Eq. 2. Hatched areas correspond to the enthalpies of respective phase transitions.

TABLE IV

Enthalpy and entropy of phase transitions in *N-p-n*-pentyloxybenzylidene-*p'-n*-butylaniline

Transition	T_c / K	ΔH / kJ mol^{-1}	ΔS / J K^{-1} mol^{-1}
crystal → smectic-G	299.69	22.68	75.70
smectic-G → nematic	325.72	7.11	21.79
nematic → isotropic liquid	342.48	1.78	5.22
		total	102.7

same as 103.4 J K^{-1} mol^{-1} for 6O · 4, in spite of the fact that the number of methylene group is less in the former compound. This situation can be accounted for in terms of the so-called odd-even effect;[19–21] the temperature

and thermodynamic quantities of phase transition are changed in zigzag way or often stepwise with the carbon number in an alkyl chain attached to a liquid crystal molecule. Therefore, if we compare the present results with those of 4O · 4 instead of 6O · 4, difference of the transition entropy, for example, might be larger.

5. GLASSY SMECTIC-G STATE

Figures 6 and 7 represent the enthalpy and entropy diagrams, respectively, which correlate the glassy and undercooled S_G states with the stable crystalline phase. The enthalpy difference between the glassy S_G and crystalline states at 0 K amounted to (10.1 ±0.1) kJ mol^{-1}; being comparable with

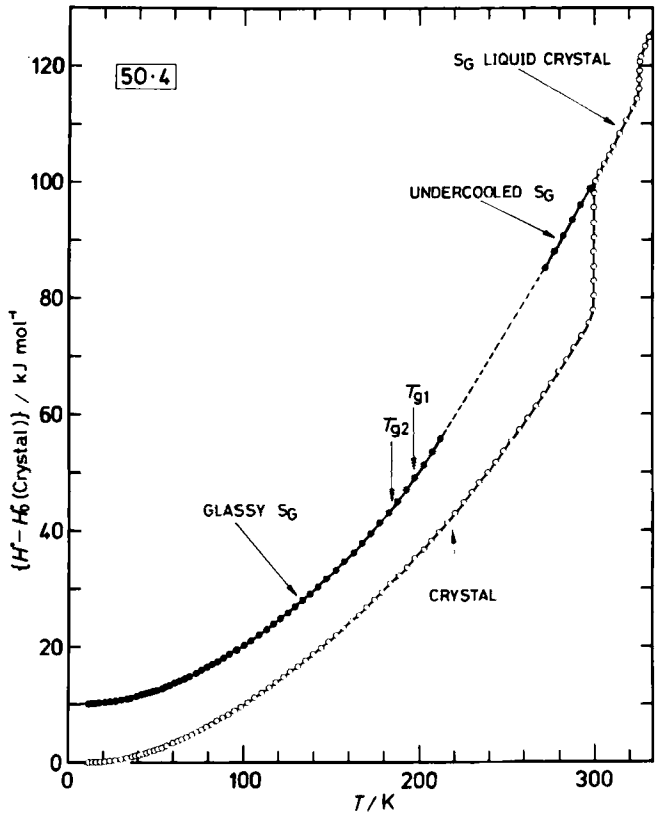

FIGURE 6 The enthalpy diagram correlating the glassy and undercooled S_G states with the stable phase of 5O · 4.

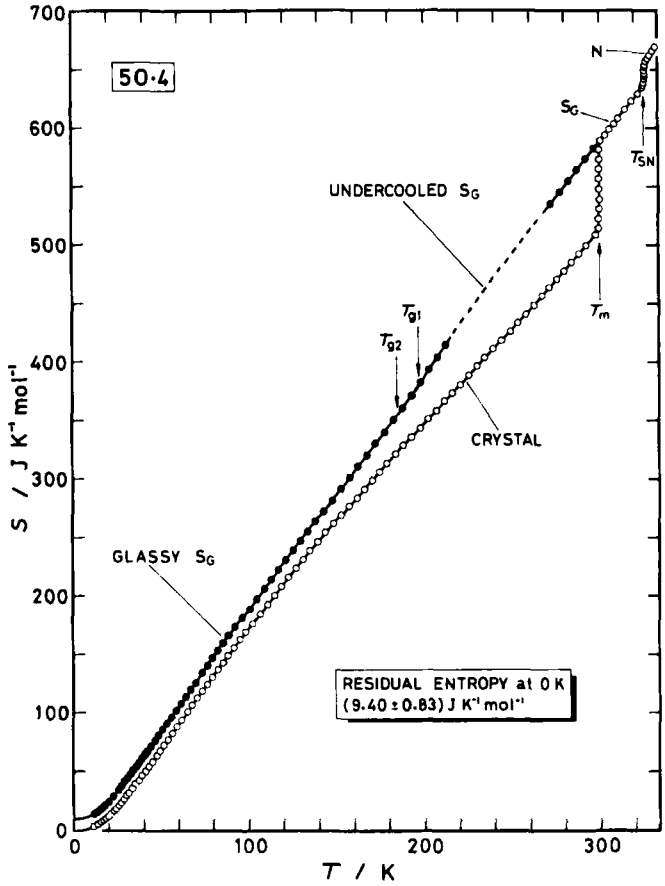

FIGURE 7 The entropy diagram correlating the glassy and undercooled S_G states with the stable phases of 5O · 4.

(9.27 ±0.16) kJ mol^{-1} for 6O · 4.[2,3] On the other hand, if we assume that the crystalline state obeys the third law of thermodynamics, the residual entropy of the glassy S_G state at 0 K becomes (9.40 ±0.83) J K^{-1} mol^{-1}. This value is somewhat large in comparison with (7.51 ±0.63) J K^{-1} mol^{-1} for the glassy S_G state of 6O · 4 but still smaller than 12.69 J K^{-1} mol^{-1} for the glassy nematic state of OHMBBA.[6] As the residual entropy is a measure of the configurational and/or conformational disorder in a glassy state, this fact reflects the situation that molecular order in the glassy state is also higher in a S_G state than in a nematic one, as in the case of stable phases.

The heat capacity of a glassy state is generally higher than that of a crystalline state. The excess heat capacities, ΔC_p(= C_p(glassy S_G)

$- C_p$(crystal)), for 5O · 4 and 6O · 4 in the range below 70 K are plotted in Figure 8. The peaks centering around 25 and 15 K are attributable to the volumetric difference between the glassy and crystalline states.[22] If a larger volume is occupied by a given amount of substance, the intermolecular forces are weakened by loose packing of molecules, which brings about a change in the frequency spectrum of normal mode vibrations and thus an increase in the heat capacity of a glassy state. It is interesting that, although the ΔC_p of 5O · 4 is much higher than that of 6O · 4 at low temperatures, the residual entropy of the former has not been sharply reduced but rather higher than the latter.

On the other hand, the ΔC_p curve of 5O · 4 above 70 K has similar form and magnitude to those of 6O · 4^3 (see Figure 9). In response to the two stepped heat capacity anomalies at around 200 K, we observed a pair of glass transition phenomena characterized by two kinds of enthalpy relaxations. Figure 10 shows the temperature dependence of the rate of enthalpy relaxation, dH/dt. Since for ordinary glass transitions only a pair of a maximum and a minimum have been detected in the dH/dt *vs* T curve, so the present results obviously indicate the existence of double glass transitions.

As this kind of double glass transition phenomenon has never been observed for nematic and cholesteric glasses, ordinary isotropic-liquid

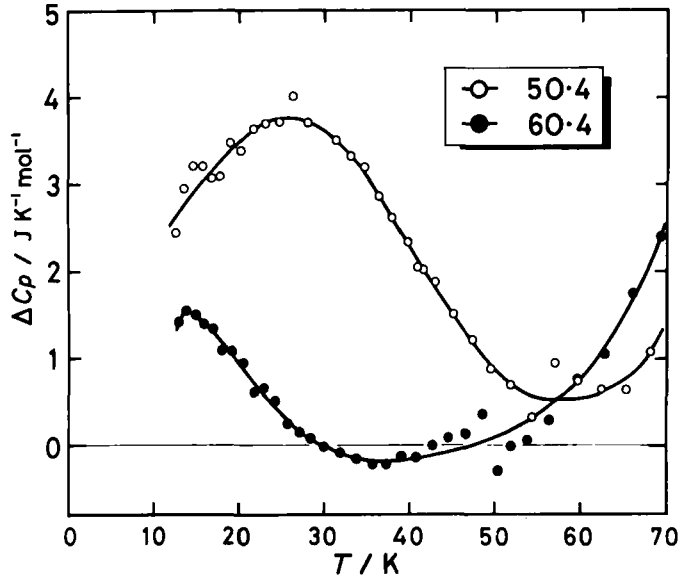

FIGURE 8 Excess heat capacities, ΔC_p ($=C_p$ (glassy S_G) $- C_p$ (crystal)), of 5O · 4 and 6O · 4 below 70 K.

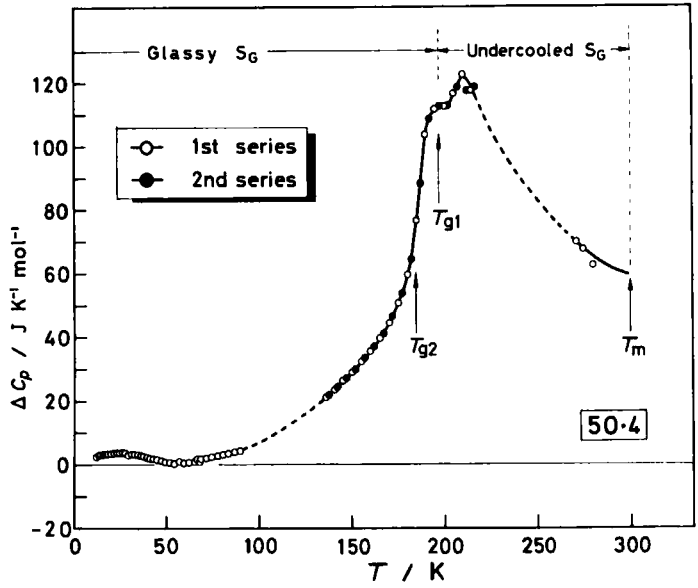

FIGURE 9 Excess heat capacities, ΔC_p ($=C_p$ (glassy or undercooled S_G) $- C_p$ (crystal)). First and second series of experiments correspond to the measurements of series 3 and 6 in Table I, respectively. T_{g1} and T_{g2} indicate the temperatures at which the relaxation times become 1 ks. As the heat capacity of the crystal exhibits an anomaly around 120 K, ΔC_p has not been plotted in this temperature region.

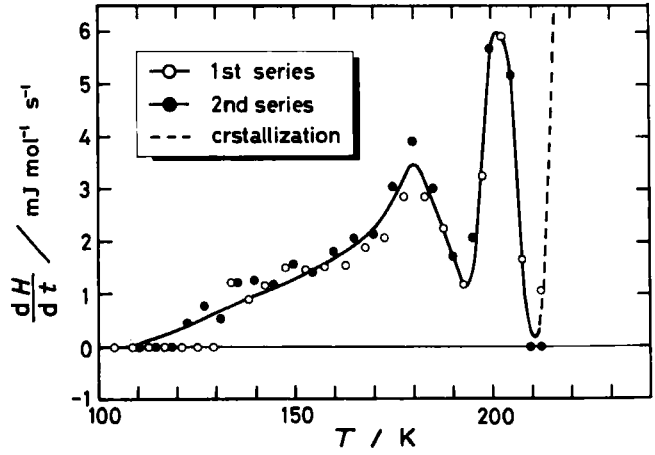

FIGURE 10 Temperature dependence of the rate of enthalpy relaxation, dH/dt, in the glass transition region. First and second series of experiments correspond to the measurements of series 3 and 6 in Table I, respectively. A broken line drawn above 220 K indicates spontaneous warming due to the transition from the undercooled S_G to the metastable crystalline states.

glasses and glassy crystals,[23,24] we thought that this phenomenon might be caused by the layer structures characteristic of smectic liquid crystals. At least, one of the double glass transitions might have its origin in a freezing of the intrinsic molecular modes of the layer structures. One of such modes is the undulation of a layer[25] and the other is anisotropic translational self-diffusion parallel and perpendicular to long molecular axes.[26,27]

To examine whether the undulation mode is a candidate for the present double glass transitions, we shall analyze the enthalpy relaxation in terms of the relaxation time as follows. Figure 11 shows a schematic diagram of the enthalpy against temperature around the glass transition region. We assumed that the enthalpy relaxation rate determined from the present experiment, $d\Delta H/dt$, is proportional to $-\Delta H/\tau$, where ΔH means a difference of the configurational enthalpy between the glassy and equilibrium states, and τ is the relaxation time. When the specimen is rapidly cooled, the first mode is frozen-in at T_{g1}, the enthalpy of which is assumed to be relaxed according to a relaxation time τ_1, while below T_{g2} the second mode having a relaxation time τ_2 is also frozen-in. As a result, the relaxation rate can be expressed as follows;

$$\left(\frac{dH}{dt}\right)_{obs} = \frac{d\Delta H_1}{dt} + \frac{d\Delta H_2}{dt} = -\frac{\Delta H_1}{\tau_1} - \frac{\Delta H_2}{\tau_2}. \tag{3}$$

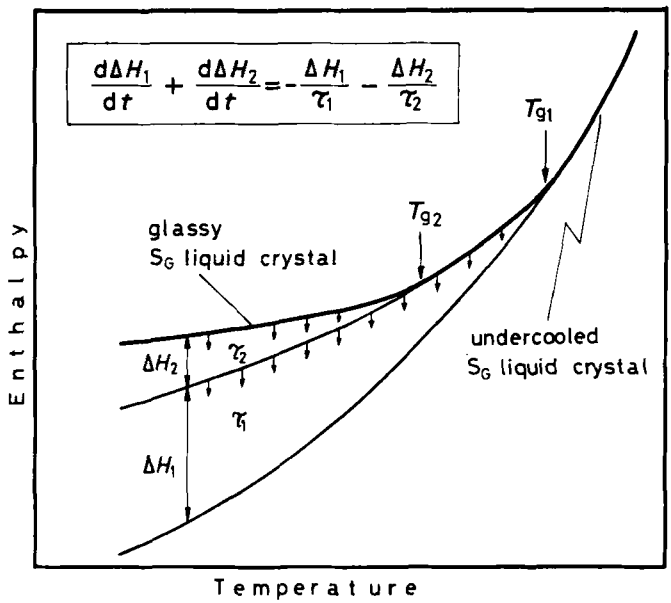

FIGURE 11 Schematic diagram of the enthalpy against temperature in the glass transition region.

As ΔH_1 and ΔH_2 can be estimated by extrapolating the configurational heat capacities below T_{g1} and T_{g2}, respectively, we can determine τ_1 and τ_2 as a function of temperature. Detailed procedures for this calculation have already been given previously.[2] Figure 12 shows the temperature dependence of τ_1 (open circles) and τ_2 (solid ones). As in the case of $6O \cdot 4^2$, the Arrhenius plots are linear at least in the glass transition region;

$$\tau_i = \tau_{0i} \exp(\Delta H_i^*/RT) \qquad (i = 1 \text{ or } 2), \tag{4}$$

where ΔH_i^* represents the activation enthalpy of the ith mode, τ_{0i} is a pre-exponential factor and R is the gas constant. If we take 1 ks of τ_i as the

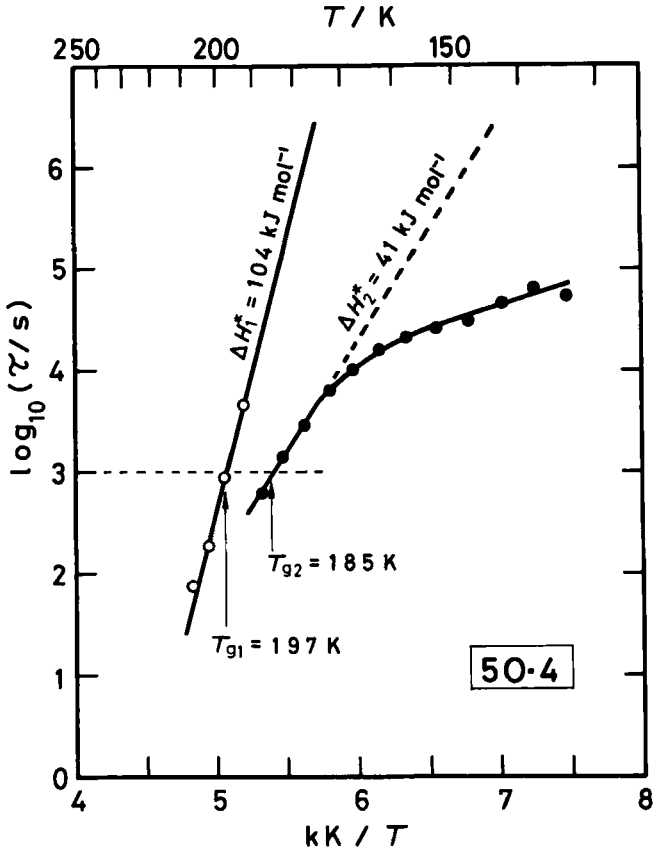

FIGURE 12 The Arrhenius plots concerning the relaxation times for the glassy S_G state of $5O \cdot 4$. Two kinds of the relaxation times, τ_1 and τ_2, are shown by open and solid circles, respectively. The glass transition temperatures, T_{g1} and T_{g2}, are taken as the temperatures at which τ_1 and τ_2 become 1 ks, respectively.

demarcation between dynamic and static disorder,[24] the Arrhenius plots given by Eq. 4 indicate that the glass transition will occur at $T_{g1} = 197$ K and $T_{g2} = 185$ K.

The only example of experiment in which thermally excited undulations of layers have been successfully observed is for the S_A phase of CBOOA on the basis of light scattering technique by Ribotta *et al.*[28] These undulation modes are highly damped and follow an exponentially decaying correlation function characteristic of a dynamic undulation. The relaxation time (or the damping rate) of layer undulations was of the order of 10^{-3} s at 75°C at which their optical experiment was done. As shown in Table V, if we extrapolate the linear Arrhenius relations (Eq. 4) to this temperature, the relaxation times of τ_2 for 5O · 4 and 6O · 4 become 3.1×10^{-3} and 1.8×10^{-3} s, respectively; very close to the damping rate found for the undulation of the smectic-A layers. Therefore, if we assume that such undulation modes also exist in the S_G state and that the undulation modes of both phases are damped in a similar time scale, it is quite likely that freezing of the undulation mode is responsible for the glass transition at T_{g2}, whereas the glass transition at T_{g1} arises from freezing of configurational modes encountered in usual glass transition phenomenon.

Alternative interpretation for the double glass transitions is the freezing of anisotropic translational self-diffusions parallel and perpendicular to long molecular axes. According to the Mössbauer effect study of the glassy states by LaPrice and Uhrich,[26,27] the Mössbauer-Debye temperatures parallel and perpendicular to the S_B layer were quite anisotropic ($\theta_\parallel = 64$ K and $\theta_\perp = 49$ K for the S_B state of BBOA (4O · 8)), while in contrast to this the glassy nematic state of MBBA (1O · 4) showed essentially isotropic values ($\theta_\parallel = \theta_\perp = 47$ K). On the other hand, in the case of the glassy S_G state of HBPA (6O · 3), as the molecules were tilted by ~43° they obtained similar values for $\theta_\parallel$ (= 46 K) and $\theta_\perp$ (= 45 K). In any case, these facts indicate that the molecular motion, probably a group self-diffusion, is easier in the direction perpendicular to the long molecular axes than in the parallel

TABLE V

The data concerning the double glass transitions found for the glassy smectic-G states. The glass transition temperatures, T_{g1} and T_{g2} are taken as those at which the relaxation times, τ_1 and τ_2, become 1 ks, respectively. ΔH^* indicates the activation enthalpy.

Compound	T_{g1} / K	ΔH_1^* / kJ mol^{-1}	τ_1(75°C) / s	T_{g2} / K	ΔH_2^* / kJ mol^{-1}	τ_2(75°C) / s
5O · 4	197	104	1.0×10^{-9}	185	41	3.1×10^{-3}
6O · 4	222	79	0.2×10^{-3}	207	56	1.8×10^{-3}

direction within a layer. Since these anisotropic molecular motions are characterized by different time scales, they may be expected to be frozen-in at different temperatures, say, T_{g1} and T_{g2}, as far as they are the candidates for the double glass transitions.

The present thermodynamic study on the glassy S_G state of 5O • 4 provided a fair evidence that the unusual glass transition phenomenon found for the S_G state of 6O • 4[2,3] is not exceptional at all but common to the smectic glasses; strictly speaking, common to the glassy S_G states for the present. The next step of study should be aimed at examination whether similar double glass transitions will occur in the smectic glasses other than the S_G state.

Acknowledgment

The authors acknowledge Itoh Science Foundation for supplying them a polarization microscope equipped with a heating stage.

References

1. M. Sorai, T. Nakamura and S. Seki, *Pramana, Suppl. 1,* 503 (1975).
2. M. Sorai, H. Yoshioka and H. Suga, *"Liquid Crystals and Ordered Fluids"* ed. A. C. Griffin and J. F. Johnson, Vol. 4, Plenum Press (1983).
3. H. Yoshioka, M. Sorai and H. Suga, *Mol. Cryst. Liq. Cryst.* (to be published).
4. K. Tsuji, M. Sorai and S. Seki, *Bull. Chem. Soc. Japan,* **44**, 1452 (1971).
5. M. Sorai and S. Seki, *Bull. Chem. Soc. Japan,* **44**, 2887 (1971).
6. M. Sorai and S. Seki, *Mol. Cryst. Liq. Cryst.,* **23**, 299 (1973).
7. J. B. Flannery, Jr. and W. Haas, *J. Phys. Chem.,* **74**, 3611 (1970).
8. G. W. Smith, Z. G. Gardlund and R. J. Curtis, *Mol. Cryst. Liq. Cryst.,* **19**, 327 (1973).
9. G. W. Smith and Z. G. Gardlund, *J. Chem. Phys.,* **59**, 3214 (1973).
10. A. Wiegeleben, L. Richter, J. Deresch and D. Demus, *Mol. Cryst. Liq. Cryst.,* **59**, 329 (1980).
11. J. W. Goodby, G. W. Gray, A. J. Leadbetter and M. A. Mazid, "Liquid Crystals of One- and Two-Dimensional Order" ed. W. Helfrich and G. Heppke, Springer, Berlin (1980), p. 3.
12. L. Verbit, *Mol. Cryst. Liq. Cryst.,* **15**, 89 (1971).
13. M. Yoshikawa, M. Sorai, H. Suga and S. Seki, *J. Phys. Chem. Solids,* **44**, 311 (1983).
14. K. Tsuji, M. Sorai, H. Suga and S. Seki, *Mol. Cryst. Liq. Cryst.,* **55**, 71 (1979).
15. M. Sorai and S. Seki, *J. Phys. Soc. Japan,* **32**, 382 (1972).
16. A. de Vries, *Pramana, Suppl.* **1**, 93 (1975).
17. L. V. Azároff, *Mol. Cryst. Liq. Cryst.,* **60**, 73 (1980).
18. A. de Vries, *Mol. Cryst. Liq. Cryst.,* **63**, 215 (1981).
19. A. J. Herbert, *Trans. Faraday Soc.,* **63**, 555 (1967).
20. H. Arnold, D. Demus, H. J. Koch, A. Nelles and H. Sackmann, *Z. Phys. Chem. (Leipzig),* **240**, 185 (1969).
21. R. D. Ennulat and A. J. Brown, *Mol. Cryst. Liq. Cryst.,* **12**, 367 (1971).
22. C. M. Guttman, *J. Chem. Phys.,* **56**, 627 (1972).
23. H. Suga and S. Seki, *J. Non-Cryst. Solids,* **16**, 171 (1974).
24. H. Suga and S. Seki, *Faraday Discussions,* **69**, 221 (1980).
25. P. G. de Gennes, *J. Phys. (Paris),* **30**, C4-65 (1969).
26. W. J. LaPrice and D. L. Uhrich, *J. Chem. Phys.,* **71**, 1498 (1979).
27. W. J. LaPrice and D. L. Uhrich, *J. Chem. Phys.,* **72**, 678 (1980).
28. R. Ribotta, D. Salin and G. Durand, *Phys. Rev. Lett.,* **32**, 6 (1974).